

INFLUENCE OF TECHNOLOGICAL AND ELECTRICAL PARAMETERS OF ESS IN CURRENT-SUPPLYING MOULD ON ELECTRODE MELTING RATE AND BASE METAL PENETRATION

V.G. SOLOVIOV and Yu.M. KUSKOV

E.O. Paton Electric Welding Institute of the NAS of Ukraine
11 Kazimir Malevich Str., 03150, Kyiv, Ukraine. E-mail: office@paton.kiev.ua

A calculation experiment was conducted which showed that the controllable electrical parameters of the ESS process can be used to regulate the metal pool shape and electrode melting rate. Dependencies between the depth of electrode deepening into the slag pool, average depth of penetration and uniformity of base metal penetration relative to average penetration depth were determined. A method was proposed for calculation of the depth of electrode deepening into the slag pool by the ratio of currents in CSM. Comparative analysis of three types of single-circuit diagrams of the mould connection to the power source was performed, and an optimum diagram for the required criteria of surfacing quality was proposed. 8 Ref., 1 Table, 12 Figures.

Keywords: *current-supplying mould, experiment, automation, metal pool, regulation, penetration, bottom plate, electrode, conductivity, diagram of power supply*

The electrostatic field generated by the potential difference between the current-carrying parts of the mould is nonuniform due to a complex configuration of inner elements of the mould and their mutual arrangement, even if to assume that the rotation of a liquid slag pool provides homogenization of its properties. First of all, the shape of equipotential surfaces of the field is affected by the value of electrode deepening into the slag pool, its diameter and shape, as well as the used type of diagram for connection of the current-supplying mould (CSM) to the power source. The intensity of electric field at each point of the slag pool determines the force and direction of the electric energy flows, which in turn determines the distribution of thermal energy at ESS, influences the electrode melting behavior, uniformity and average penetration depth of product and also the character of a liquid metal crystallization. The problems of mathematical modeling of electrical parameters of electroslag processes were given attention in many works, for example [1–4], however, there are almost no works on modeling and studying the influence of electrical parameters on the uniformity and average penetration depth of product at ESS in current-supplying mould.

In the work [5], as a result of modeling the electric field in slag pool in the CSM on electrically conductive paper, the authors made the conclusion that a middle section of the mould, due to its electrical

conductivity, shunts a part of the slag pool, shifts the region of prevailing heat release into the near-wall region of the mould, leaving a central zone to be relatively cold. However, directly at the mould wall itself, the metal pool remains cold due to the mould water cooling and, due to that, the pool can acquire a specific form of «sombbrero».

The authors of the work [6] make a conclusion that varying the values of currents passing to the electrode and mould during surfacing using a «potential» electrode, it is possible to significantly change the shape of the metal pool bottom: from the concave cone-shaped, characteristic for the conventional ESR process, to the convex one in the central part of the deposited layer, inherent in surfacing without electrode.

The aim of the work is to perform mathematical modeling of distribution of the slag pool potential in the CSM by using the PDETool MATLAB package and to conduct a calculation experiment, which will answer the following questions:

- how to use the controllable electrical parameters to regulate the metal pool shape and the electrode melting rate;
- how the value of electrode deepening into the slag pool affects the average penetration depth of product and the uniformity of penetration relative to the average penetration depth;

- how to use the values of the controllable electrical parameters to calculate the value of electrode deepening into the slag pool;
- which single-circuit diagram (of three types) of the mould connection to the power source is the most optimal for solution of the put problem;
- in which cases it is necessary to use the CSM power supply diagram: single- or two-circuit diagram.

One of the standard boundary value problems in PDETool [7] is the electrostatic problem, which was used in this work, since the subject of study was the distribution of electric field intensity in a slag pool between the electrode surfaces, graphite lining of a current-carrying section of the mould and the bottom plate, to which the potential was applied.

In the proposed statement of the problem, it was assumed that the object has an axial symmetry. Therefore, the two-dimensional model is represented in a cylindrical coordinate system. Moreover, the rotation of the molten slag pool around the mould axis provides an axial homogenization of its properties. We assume that there is a qualitative effect of the electrostatic field and its nonuniformity near the surface of the bottom plate (product) on the nonuniformity and penetration depth of the upper layer of the product in accordance with the Joule–Lenz law. The boundary conditions of the slag pool surface and the forming section of the mould are taken in accordance with the conditions of the Neumann problem, while those for the boundaries of the electrode surfaces, the mould graphite bushing and the bottom plate were taken in accordance with the Dirichlet problem conditions.

The accepted model and the carried out calculation experiment do not pretend to obtaining numerical interrelations of input and output variables which could be used in surfacing, but allow evaluating the qualitative relationship of the mentioned variables, correctly planning and simplifying the experimental surfacing to obtain the quantitative interrelations.

The equation of electrostatics with respect to a scalar electric potential is

$$-\operatorname{div}(\varepsilon \nabla V) = \rho \varepsilon_0,$$

where ε is the relative dielectric permeability of the medium; $\varepsilon_0 = 8.85 \cdot 10^{-12}$ F/m is the absolute dielectric permeability of vacuum (basic electric constant); V is the scalar electric potential; ρ is the scalar field of the volumetric density of electric charge.

The value of relative dielectric permeability of slag is accepted as $\varepsilon = 70$. In connection with the lack of data on this parameter in the literature, the value ε for this parameter is assumed equal to the relative dielectric permeability of sea water. To solve the boundary value problem of Dirichlet $r = hV$ (where r is the

electric potential; h is the weight coefficient), the value $h = 1$, and the value of the scalar electrical potential $V = 100$ of conventional units were accepted, which provides the evaluation of voltages between the equipotential lines in a percentage relation. To solve the Neumann boundary value problem $\varepsilon \nabla V + qV = g$, q is the coefficient determining the influence of V value in the model, taken equal to 0.7, and g is the charge on side surfaces of a forming section of the mould, is accepted as equal to $<10^{-10}$ C, i.e. $g = 0$. For a slag pool $\rho = 0$. Visualization of scalar elliptic PDEs allowed using the «method of graphic images», which is successfully applied in the calculation of fields of charged bodies, located near plane or cylindrical conducting surfaces [8].

Problem statement. As a result of modeling, it is necessary to determine the nature of effect of values of the electrode diameter d_e , the electrode deepening into the slag pool h_d , the level of the metal pool h_m relative to the level of the lower edge of the current-carrying section of the mould on the controllable electrical parameters of ESS in CSM.

The geometric characteristics and constants of the model are:

- inner diameter of the mould forming part is 180 mm;
- cylindrical electrode of diameter d_e : 40 (a), 90 (b) and 130 mm (c);
- two-section mould (without middle section);
- height of graphite lining wetted with slag (wet part), 20 mm;
- distance from the bottom edge of graphite lining to the metal pool mirror h_m : 30 (a), 50 (b) and 80 mm (c). The depth of the slag pool is, respectively, h_s : 50 (a), 70 (b) and 100 mm (c).
- value of electrode deepening into the slag pool h_d : 10 (a), 20 (b) and 40 mm (c).

Figure 1 shows the examples of models of electrostatic fields for CSM with different diagrams of connections to the source, different diameters of electrodes, with different depths of slag pool and different values of electrode deepening.

There are three types of diagrams for connecting the elements of the working zone of the mould (WZM) to the power source (PS) — the diagram using the «potential» electrode (type «E») in Figure 2, a, the diagram using the «potential» mould (type «M») in Figure 2, b and the diagram using the «potential» bottom plate (type «B») in Figure 2, c.

Calculations of currents of the bottom plate, electrode and mould at the diagram using a «potential» bottom plate (type «B»). With the diagram of CSM supply of type «B» the highest current passes through the bottom plate, which is equal to the sum of currents

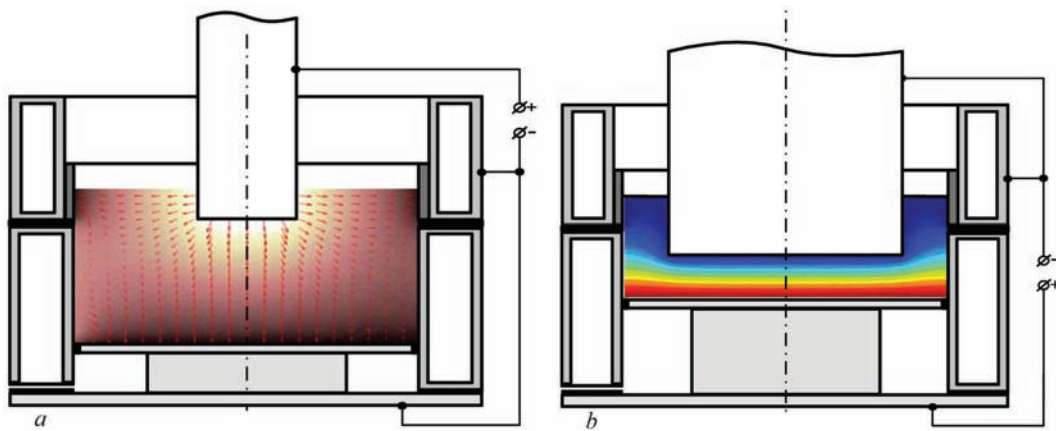


Figure 1. Examples of calculation of intensity of electric field and field with equipotential lines: *a* — for CSM, switched-on according to the diagram with a «potential» electrode, $d_e = 40$ mm, $h_s = 100$ mm and $h_d = 20$ mm; *b* — for CSM, switched-on according to the diagram with a «potential» bottom plate, $d_e = 130$ mm, $h_s = 70$ mm and $h_d = 40$ mm

passing through the electrode and mould. In this way, the best heating of product is provided, but the efficiency of melting the electrode is lower than, for example, in connecting CSM to the source according to the diagram with a «potential» electrode (type «E»).

Figure 3 shows the calculated values of the currents of the bottom plate I_b , electrode I_e , and mould I_m depending on the value of electrode deepening h_d and on the electrode diameter d_e , at the slag pool depth $h_s = 100$ mm.

As is seen from the diagram of Figure 3, *a*, the electrode current I_e during deepening into a slag pool is increased almost in the proportion to the value of deepening, since the slag pool conductivity is increased with increasing the area of the «wet» part of electrode and the distance from the electrode to the product, and also with increasing d_e . During deepening the electrode, the current of the mould I_m decreases, it is affected by «screening» of the graphite lining of electrode, which has the same potential as

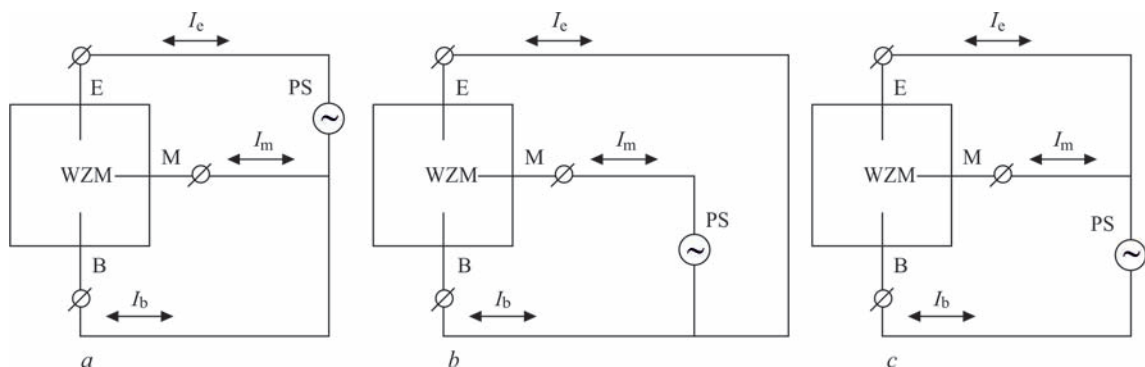


Figure 2. Diagrams of connecting the elements of working zone of mould to the power source with the use of: *a* — potential electrode (type «E»); *b* — potential mould (type «M»); *c* — potential bottom plate (type «B»)

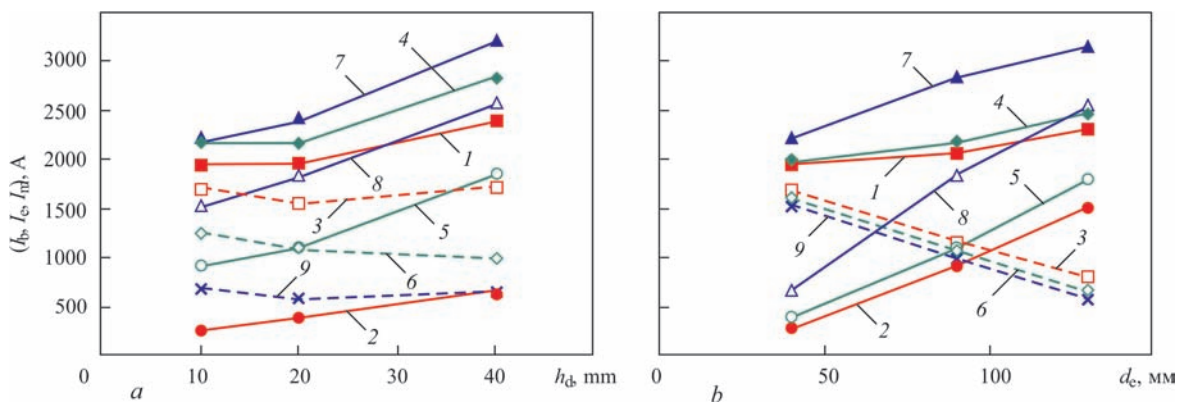


Figure 3. Changes of currents of bottom plate I_b , electrode I_e and mould I_m depending on: *a* — value of electrode deepening h_d : 1, 2, 3 — I_b, I_e, I_m , respectively (at $d_e = 40$ mm); 4, 5, 6 — I_b, I_e, I_m , respectively (at $d_e = 90$ mm); 7, 8, 9 — I_b, I_e, I_m , respectively (at $d_e = 130$ mm); *b* — diameter of electrode d_e , at the depth of slag pool $h_s = 100$ mm: 1, 2, 3 — I_b, I_e, I_m , respectively (at $h_d = 10$ mm); 4, 5, 6 — I_b, I_e, I_m , respectively (at $h_d = 20$ mm); 7, 8, 9 — I_b, I_e, I_m , respectively (at $h_d = 40$ mm)

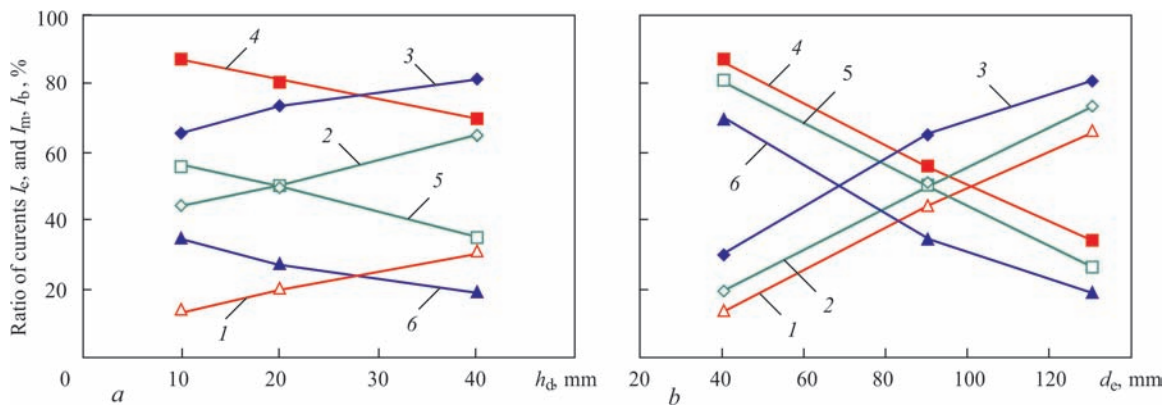


Figure 4. Changes of percent ratio of electrode currents I_e and the mould I_m to the bottom plate current I_b depending on: *a* — value of electrode deepening h_d : 1–4 — I_e/I_b , I_m/I_b , respectively (at $d_e = 40$ mm); 2, 5 — I_e/I_b and I_m/I_b , respectively (at $d_e = 90$ mm); 3, 6 — I_e/I_b and I_m/I_b , respectively (at $d_e = 130$ mm); *b* — diameter of electrode d_e , at the depth of slag pool $h_s = 100$ mm: 1–4 — I_e/I_b and I_m/I_b , respectively (at $h_d = 10$ mm); 2, 5 — I_e/I_b and I_m/I_b , respectively (at $h_d = 20$ mm); 3, 6 — I_e/I_b and I_m/I_b , respectively (at $h_d = 40$ mm)

the graphite lining, and which during deepening into the slag pool and approaching a product, undertakes a greater percentage of the source total current. With deepening the electrode, the current of the bottom plate I_b increases. It should be taken into account that I_m and I_e at $d_e = 90$ mm are close in values, and at deepening to 20 mm, they are even equal. At $d_e = 40$ mm, the current of the mould I_m exceeds the current of the electrode I_e , and at $d_e = 130$ mm, we observe the other situation: the electrode current exceeds the mould current. From the diagram in Figure 3, *b*, a weak influence of the electrode diameter d_e on the current of bottom plate I_b and its strong influence on I_e and I_m are seen at the small deepening of the electrode.

At the diagrams of Figure 4, *a*, it is seen that for $h_d = 10$ mm, the current of the mould prevails over the electrode current only at $d_e < 100$ mm, at $d_e > 100$ mm the situation changes to the opposite one. For $h_d = 20$ mm, the mould current prevails over the electrode current at $d_e < 90$ mm, at $d_e > 90$ mm the situation changes to the opposite one. For $h_d = 40$ mm, the mould current prevails over the electrode current at $d_e < 70$ mm, at $d_e > 70$ mm the situation changes to the opposite one.

At the value of the depth of the slag pool $h_s = 100$ mm from the diagrams in Figure 4, *b*, it is seen that at $d_e = 40$ mm over the entire range of changes h_d , the mould current has a greater effect on the process as compared to the current of the electrode. At $d_e = 90$ mm at $h_d > 20$ mm, the current of the electrode prevails over the current of the mould. At $d_e = 130$ mm over the entire range of changes in h_d , the current of the electrode has a greater effect on the process as compared to the mould current.

Obviously, that for ESS in CSM, the electrode current determines its melting rate, the current of the mould plays the role of equalizing the electric field near the product and the bottom plate current deter-

mines the penetration depth of the product, i.e. using such diagrams as in Figure 3, it is possible to choose the necessary ratio between the size of the electrode deepening and its diameter.

As is seen from the diagrams in Figure 5 the change in the ratio of currents of the electrode I_e to the mould current I_m from the deepening of the electrode h_d has a pronounced character and corresponds to a practically linear dependence. So, according to the value I_e/I_m , it is possible indirectly to calculate such a parameter as the value of deepening h_d and to use it for regulating the ESS process. Moreover, the ratio of the currents I_e/I_m should be much less dependent on the change in the slag conductivity due to the change in temperature, than the currents of the electrode and the mould themselves.

Calculation of parameters of electrostatic field near the slag pool bottom (type «B»). The distribution of the electric field intensity over the product surface characterizes the distribution of current den-

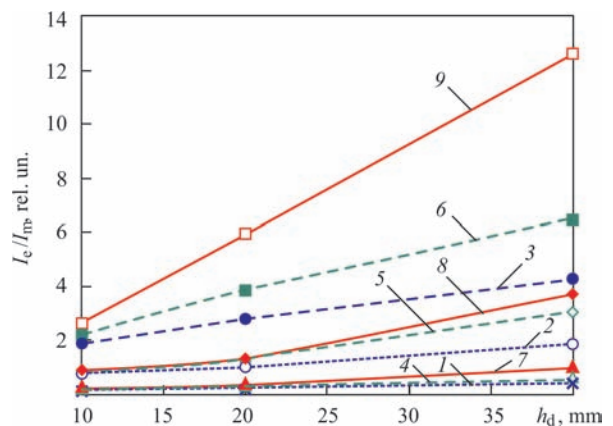


Figure 5. Changes in the ratio of electrode currents I_e to mould current I_m , depending on deepening of the electrode h_d at different electrode diameters for different depths of the slag pool h_s : 1, 2, 3 — I_e/I_m (for $d_e = 40, 90, 130$ mm, respectively, at $h_s = 100$ mm); 4, 5, 6 — I_e/I_m (for $d_e = 40, 90, 130$ mm, respectively, at $h_s = 70$ mm); 7, 8, 9 — I_e/I_m (for $d_e = 40, 90, 130$ mm, respectively, at $h_s = 50$ mm)

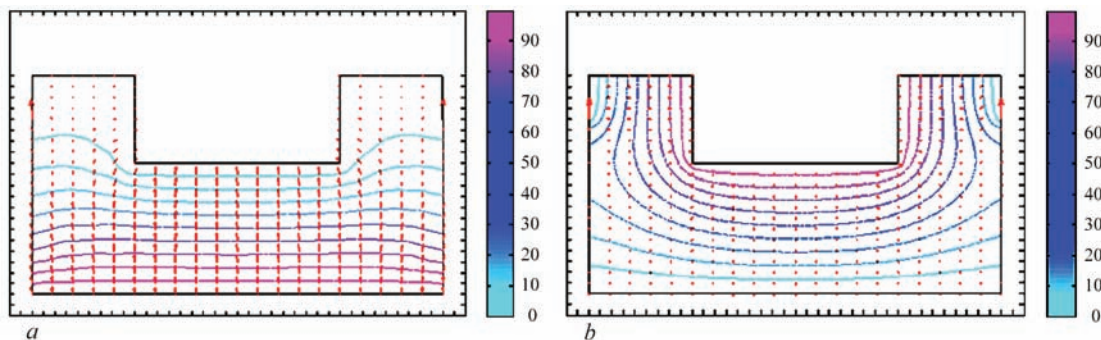


Figure 6. Calculation of shape of equipotential line of electrostatic fields in the vicinity of the slag pool bottom at the electrode deepening $h_d = 40$ mm and the diameter of electrode $d_e = 90$ mm for the depth of slag pool $h_s = 100$ mm; *a* — diagram of connection of type «B»; *b* — diagram of connection of type «E»

sity and, thus, the relative distribution of the thermal field over the metal pool surface. So, according to the shape of the equipotential lines of the model in the product vicinity, it is possible to predict the relative nonuniformity of penetration δ_p , as well as the relative average surface penetration depth of product \bar{h}_p .

Figure 6 shows an example of calculating the shape of equipotential lines of electrostatic fields near the slag pool bottom during connection of CSM to the source according to the diagram of type «B» and type «E». As is seen in Figure 6, *a*, near the bottom of slag pool (or on the surface of product) for the connection diagram of type «B», the electric field intensity in the near-wall region of mould is higher than in the product center. The opposite ratio between the intensities is seen while using the connection diagram of type «E».

The relative nonuniformity of penetration δ_p was calculated by the formula:

$$\delta_p = \frac{\sqrt{\frac{1}{n} \sum_{i=1}^n (h_{pi} - \bar{h}_p)^2}}{\bar{h}_p}$$

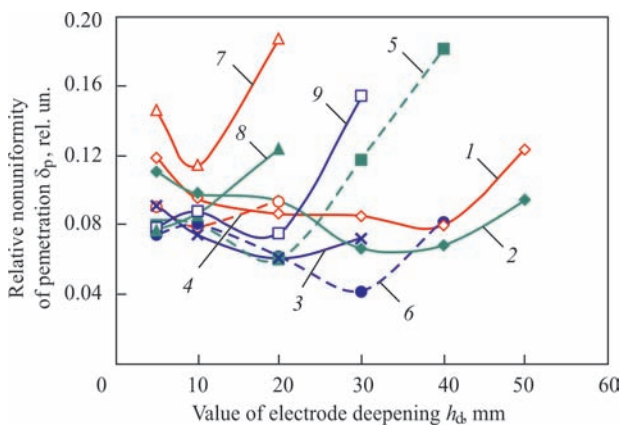


Figure 7. Changes in the relative nonuniformity of penetration δ_p depending on electrode deepening h_d at different diameters of electrode d_e for different depths of slag pool h_s : 1, 2, 3 — δ_p (for $d_e = 40, 90, 130$ mm, respectively, at $h_s = 100$ mm); 4, 5, 6 — δ_p (for $d_e = 40, 90, 130$ mm, respectively, at $h_s = 70$ mm); 7, 8, 9 — δ_p (for $d_e = 40, 90, 130$ mm, respectively, at $h_s = 50$ mm)

where the number of measuring points along the mould diameter $n = 19$; h_{pi} is the relative penetration depth at the i -th point of measurement, inversely proportional to the distance between the neighboring equipotential lines along the i -th coordinate.

From the diagrams in Figure 7 it is seen that the dependences δ_p on h_d for different diameters of electrodes and the slag pool depths are of extreme nature in the investigated range of h_d changes. The minimum value of the relative penetration depth is observed for $d_e = 130$ and $h_s = 70$ mm at the value of electrode deepening into the slag pool $h_d = 30$ mm.

The diagrams of change in the relative average penetration depth \bar{h}_p depending on the electrode deepening h_d at different diameters of electrode d_e for different slag pool depths h_s are shown in Figure 8. Here we observe that with increase in the deepening of the electrode into the slag pool, that is, when it approaches the product, the average penetration depth of the product grows. An increase in the electrode diameter, as well as a decrease in the slag pool depth, leads to increase in the average penetration depth.

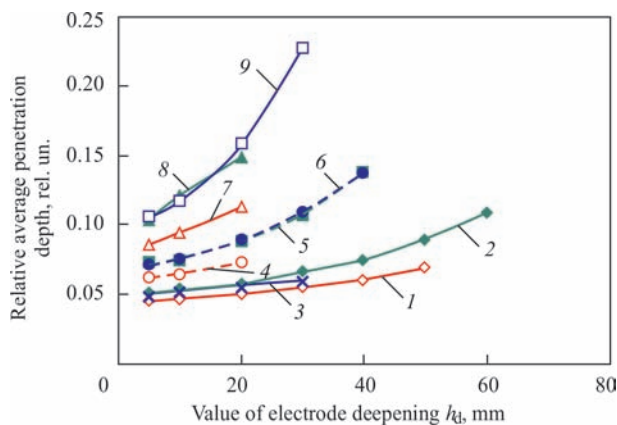


Figure 8. Changes in the relative average penetration depth \bar{h}_p depending on electrode deepening h_d at different diameters of electrode d_e for different slag pool depths h_s : 1, 2, 3 — \bar{h}_p (for $d_e = 40, 90, 130$ mm, respectively, at $h_s = 100$ mm); 4, 5, 6 — \bar{h}_p (for $d_e = 40, 90, 130$ mm, respectively, at $h_s = 70$ mm); 7, 8, 9 — \bar{h}_p (for $d_e = 40, 90, 130$ mm, respectively, at $h_s = 50$ mm)

Figure 9 shows the diagrams of change in the minimum values of relative non-uniformity of penetration δ_p , depending on the slag pool depth h_s for different diameters of electrodes d_e . It follows from the diagrams that the optimum depth of the slag pool lies in the range of 70–80 mm, and the best value $\delta_p = 0.04$ is in the process with electrode $d_e = 130$ mm.

The similar calculation experiments were carried out for ESS in CSM according to the diagram of connection to the power source with a «potential» electrode (type «E») and with a «potential» mould (type «M»). The volume of this paper does not allow providing all the data obtained from these experiments, so we will present only the generalized results:

1. In the diagram of CSM connection to the power source of type «E», the highest current is passed through the electrode, which is equal to the sum of currents, passing through the bottom plate and mould. Thus, the more effective electrode melting and sufficient heating of product are provided as compared to the connection of «B» type diagram. ESS with CSM connected according to the diagram «E» will have the highest efficiency as compared to the «B» and «M» type connections. The dependence of the ratio of current of the bottom plate I_b to the current of the mould I_m on deepening of the electrode h_d has an essentially nonlinear nature, approaching the exponential one. Nevertheless, this circumstance can not affect the use of the functions $h_d = F[I_b/I_m]$ for indirect measurement of deepening value and automatic maintenance of the preset value of this parameter. The same as in the diagram of type «B», with increase in electrode deepening into the slag pool, i.e. at its approaching to the product, the average penetration depth of the product is increased. An increase in the electrode diameter as well as a decrease in the slag pool depth, leads to increase in the average penetration depth. The optimum depth of the slag pool, at which the nonuniformity of penetration δ_p is minimum, corresponds to $h_d = 100$ mm, and the best value $\delta_p = 0.06$ will be for the process with the electrode diameter $d_e = 130$ mm.

2. Connecting the CSM to the power source according to the diagram of «M» type is less widespread in practice, as far as the current passing through the mould is the sum of currents of the electrode and bottom plate, due to which the electrode melting efficiency and the role of the bottom plate, heating the product, are decreased. Dependence of the ratio of the electrode current I_e to the bottom plate current I_b on the deepening the electrode h_d has a clearly distinct character and can be used for indirect measuring the value of electrode deepening into the slag pool. The dependences δ_p on h_d for the diagram of type «M» for CSM connection to the power source do not have an

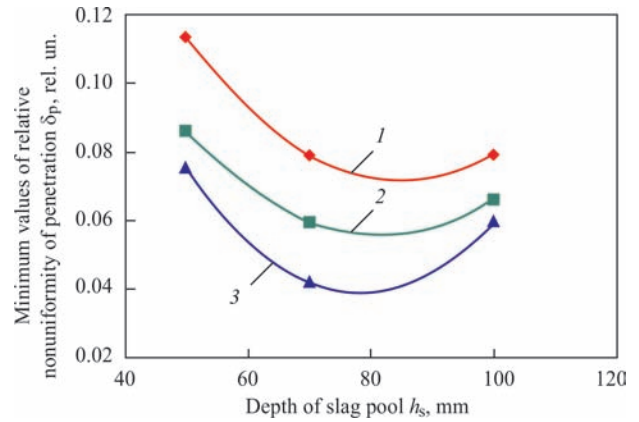


Figure 9. Changes in the minimum values of the relative non-uniformity of penetration δ_p depending on the slag pool depth h_s at different electrode diameters d_e : 1, 2, 3 — δ_p (for $d_e = 40, 90, 130$ mm, respectively)

extreme character, they sharply elevate during electrode deepening, and the values δ_p exceed the values obtained for the connection diagrams of type «B» and «E» by an order. With an increase in electrode deepening into the slag pool, i.e. when it approaches the product, the average penetration depth of the product almost does not change. An increase in the electrode diameter, as well as a decrease in the slag pool depth, leads to an increase in the average penetration depth. The optimum depth of the slag pool for minimizing the nonuniformity of penetration δ_p corresponds to $h_d = 100$ mm, and the best value $\delta_p = 0.5$ will be for the process with the electrode diameter $d_e = 40$ mm.

3. The Table shows calculations of the consumed power ΣP for ESS at $d_e = 90$ mm, $h_d = 20$ mm, $h_s = 100$ mm for three types of connection circuits, under the condition that the same power $P_e = 99.950$ kW is consumed at the electrode for all the cases considered. It is seen from the calculations that the process during connection according to the diagrams of type «B» and «M», consumes approximately 1.6 times more power than that in the diagram of type «E».

Simulation of two-circuit diagram of CSM supply with a «potential» bottom plate diagram of connection (type «B»). The use of two power sources for carrying out the process of ESS with CSM is considered to be less economical and more cumbersome than supply by one source. However, the use of two-circuit diagram of CSM supply can lead in some

Consumed power at ESS for different connection diagrams

Power consumption, kW	Type of connection diagram		
	«B»	«E»	«M»
P_e	99.950	99.950	99.950
ΣP	162.456	99.950	162.540
$\Sigma P/P_e$	1.63	1.0	1.63

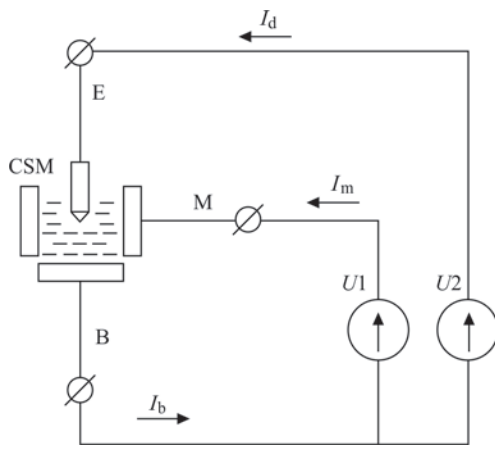


Figure 10. Two-circuit diagram of CSM supply: E, M and B — terminals for connection to the electrode, current-carrying section of mould and bottom plate, respectively; I_e , I_m and I_b — current of the electrode, current of the mould and current of the bottom plate, respectively; sources of direct current with voltages $U1$ and $U2$, respectively

cases to an improvement in the penetration characteristics of product.

During simulation of two-circuit diagram of CSM supply, a situation was considered where the voltage of the electrode varies with respect to the mould voltage. In this case, the voltage of the mould remains unchanged. In this case, we investigate the changes in the relative average nonuniformity of penetration δ_p during the hypothetical transition of the power circuit from the diagram of type «B» to the diagram of type «M», namely, the change in δ_p with an increase in the role of mould in the product penetration.

Figure 10 shows a two-circuit diagram of CSM supply. The voltage at the mould relative to the bottom plate $U1$ remains unchanged in calculations, and the voltage at the electrode relative to the bottom plate $U2$ is gradually reduced from the value equal to $U1$, i.e. $U1/U2 = 1$ to the value $U1/U2 = 4$.

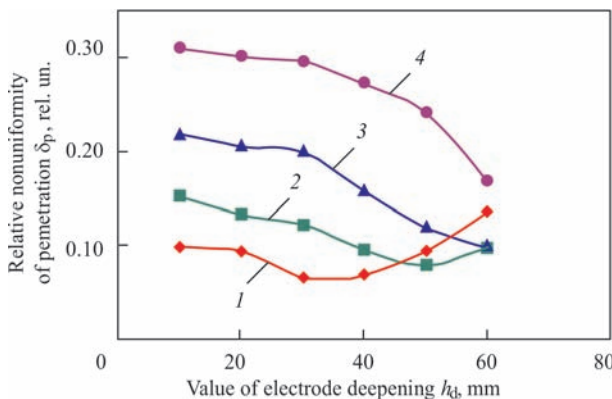


Figure 11. Changes in the relative nonuniformity of penetration δ_p , depending on deepening of the electrode h_d at different voltage ratios on the mould and the electrode $U1/U2$ with an electrode diameter $d_e = 90$ mm and depth of the slag pool $h_s = 100$ mm: 1 — $U1/U2 = 1$; 2 — 1.5; 3 — 2.33; 4 — 4

The calculation diagrams of the change in relative nonuniformity of penetration δ_p depending on deepening the electrode h_d at different ratios of voltages at the mould and the electrode $U1/U2$ at the electrode diameter $d_e = 90$ mm and the depth of the slag pool $h_s = 100$ mm are shown in Figure 11.

From Figure 11 it is seen that in the investigated range of the value of the electrode deepening, the best values of δ_p will be at the equality of $U1$ and $U2$. When $U1$ and $U2$ are equal, the two-circuit diagram is almost a single-circuit one. However, when the electrode is deepened to more than 45 mm and the ratio of $U1/U2 = 1.5$, the two-circuit diagram has lower values of δ_p than that at the single-circuit diagram of connection.

The calculations of parameters of the electrostatic field near the slag pool bottom allowed getting an idea of its shape. For example, Figure 12 shows the calculation distribution of the relative current density I_b along the radius of the product R_b for different values of electrode deepening h_d with a diameter $d_e = 90$ mm (connection diagram of type «E»). The distribution of current density of the bottom plate determines the shape of the metal pool bottom.

Generalization of calculation experiment results.

1. With the help of calculation experiment, it was found that the main parameters of surfacing by the electrode of a large cross-section (depth and uniformity of penetration) are determined both as the technological parameters (electrode diameter and its deepening into the slag pool of different depth, the number of power sources and the diagram of CSM connection to them), and also as controllable electrical indicators of the process corresponding to these parameters.

2. It was confirmed that the values I_e/I_m for the diagram of type «B», I_b/I_m for the diagram of type «E» and I_e/I_m for the diagram of type «M», which can be obtained by calculation in the process of surfacing, correspond to such an important parameter as the value of the electrode deepening. The automatic mainte-

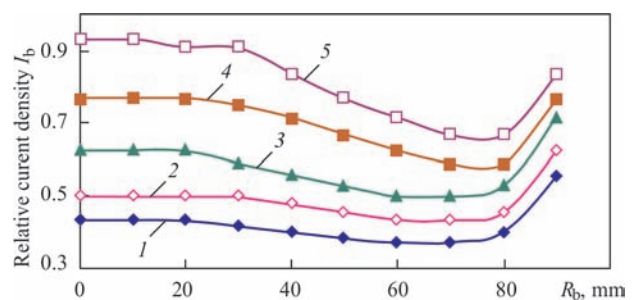


Figure 12. Distribution of relative current density I_b along the radius of the product R_b for different values of deepening of the electrode h_d with a diameter $d_e = 90$ mm (connection diagram of type «E»): 1 — $h_d = 10$; 2 — 20; 3 — 30; 4 — 40; 5 — 50 mm

nance of the preset value of the electrode deepening will provide the necessary uniformity and penetration depth of the product.

3. A comparative analysis of three types of circuits of CSM connection to the power source was carried out, which revealed that the supply circuit of type «B» provides the least nonuniformity of penetration at the minimum penetration depth of the product, and the diagram of type «E» provides a good electrode melting, i.e. the improved process efficiency with acceptable nonuniformity and penetration depth of the product. In ESS with CSM, this gives grounds to use the diagram of type «B» and then the diagram of type «E» at the initial stage of the process. The switching of circuits should be performed automatically.

4. Analysis of the model with a two-circuit diagram of connection did not show special advantages in the quality of penetration at the process using a CSM single-circuit diagram of CSM supply.

1. Troyansky, A.A., Ryabtsev, A.D., Samborsky, M.V., Mastepan, V.Yu. (2002) Application of measuring information system for investigation of ESR process. *Metall i Litio Ukrainu*, **7–8**, 25–26 [in Russian].
2. Troyansky, A.A., Ryabtsev, A.D., Mastepan, V.Yu. (2004) Indirect methods for control of ESR technological parameters based on application of harmonic composition of current and voltage of remelting. In: *Abstr. of Papers of Int. Scient. Conf. on Modern Problems of Theory and Practice of Quality Steel Production (Mariupol, 8-10 September 2004)*. Priazov. STU, 80–82.
3. Troyansky, A.A., Ryabtsev, A.D., Mastepan, V.Yu. et al. (2005) Application of method of current distribution modeling as the base for development of technology of high-quality ingots by CESR method. *Metallurg. Protsessy i Oborudovaniye*, **2**, 25–27 [in Russian].
4. Makhnenko, V.I., Demchenko, V.F., Tarasevich, N.I., Krikent, I.V. (1985) Calculation system for investigation of current distribution in slag pool. *Problemy Spets. Elektrometallurgii*, **1**, 14–19 [in Russian].
5. Tomilenko, S.V., Kuskov, Yu.M. (2000) Regulation and stabilization of base metal depth penetration in electroslag surfacing in current-supplying mold. *Svarochn. Proizvodstvo*, **9**, 32–35 [in Russian].
6. Tomilenko, S.V., Kuskov, Yu.M. (1999) Power features of electroslag process in current-supplying mold. *Avtomatich. Svarka*, **2**, 51–53 [in Russian].
7. Shmelev, V.E. Partial differential equations toolbox. Toolbox for solution of differential equations in partial derivatives [in Russian]. <http://matlab.exponenta.ru/pde/book1/index.php>
8. Govorkov, V.A. (1968) *Electric and magnetic fields. 3rd Ed.* Moscow, Energiya [in Russian].

Received 30.03.2018